J Soils Sediments (2011) 11:562–576
DOI 10.1007/s11368-011-0339-2

SOILS, SEC 1 • SOIL ORGANIC MATTER DYNAMICS AND NUTRIENT CYCLING • RESEARCH ARTICLE

Modeling impacts of climate change on carbon dynamics in a steppe ecosystem in Inner Mongolia, China

Xiaoming Kang · Yanbin Hao · Changsheng Li · Xiaoyong Cui · Jinzhi Wang · Yichao Rui · Haishan Niu · Yanfen Wang

Received: 10 September 2010 / Accepted: 20 January 2011 / Published online: 22 February 2011

Abstract
Purpose In this study, a process-oriented biogeochemistry model, denitrification–decomposition (DNDC), was employed and adapted to interpret and integrate the field observations that the tested ecosystem was a weak sink of atmospheric carbon dioxide (CO_2) in 2004 but a strong source in 2005 during the growing seasons. Then we applied the model to predict long-term impacts of climate change on carbon (C) dynamics in the semiarid grassland.
Materials and methods To adapt DNDC for the targeted grassland, we modified the default values of several grass parameters such as maximum biomass production, biomass partitions, plant tissue C/N ratio, and accumulative thermal degree days based on local observations. Daily weather data for 2004 and 2005 in conjunction with soil properties and management practices for the location were utilized as inputs to simulate the grass growth and soil C dynamics. The modeled C fluxes were compared with the eddy tower data. Sensitivity tests were conducted with a baseline and twelve alternative climate scenarios of 100 years for the target grassland.
Results and discussion The observed and modeled CO_2 fluxes data were well in agreement ($P<0.0001$), both showing that the grassland shifted from a sink to a source of atmospheric CO_2 from a wet year (2004) to a dry year (2005) over growing season. Simulations of 100 years found that, under the fenced conditions, (1) the tested ecosystem would gain C with the baseline climate conditions at a rate of 200 kg C/ha/year; (2) the warmer and drier climate scenario made the worst case having the lowest grass production with 72 kg C/ha/year lost from the soil carbon pool; and (3) the cooler and wetter climate scenario made the best case having the highest biomass production with 790 kg C/ha/year sequestered in the soil during the simulated 100 years.
Conclusions DNDC model could be used for the prediction of C dynamics in this semiarid grassland ecosystem. Since the ecosystem production is precipitation-limited, a cooler or wetter future climate would substantially elevate the C sequestration capacity of the grassland. However, the C sequestration potential could significantly decrease and even become negative to turn the ecosystem to a source of atmospheric CO_2 if the climate turned to be warmer and/or drier in the coming 100 years.

Keywords Climate change · Carbon flux · DNDC · Eddy covariance · Grassland

Responsible editor: Gilbert Sigua

X. Kang · J. Wang · Y. Rui · H. Niu
College of Resources and Environment,
Graduate University of Chinese Academy of Sciences,
Beijing 100049, People's Republic of China

Y. Hao · X. Cui · Y. Wang (✉)
College of Life Sciences,
Graduate University of Chinese Academy of Sciences,
Beijing 100049, People's Republic of China
e-mail: yfwang@gucas.ac.cn

C. Li
Institute for the Study of Earth, Ocean and Space,
University of New Hampshire,
Durham, NH, USA

1 Introduction

As one of the most widespread vegetation types on the global land surface, grasslands play an important role in the global carbon (C) budget, with C pools sensitive to climate change (Fan et al. 1998; Hunt et al. 2004; Sims and Bradford 2001; Sundquist 1993; Tans et al. 1990). A recent

report (IPCC 2007) states that human activities since the industrial revolution have contributed to global and regional climate change by raising global mean temperature and changing precipitation regimes and that grassland C cycles are significantly coupled with climate change and highly sensitive to climate variation. A number of studies have indicated that grasslands could take up more C under moist climate conditions at the ecosystem scale (Meyers 2001; Nagy et al. 2007; Suyker et al. 2003; Xu and Baldocchi 2004; Zhang et al. 2010). However, studies are relatively sparse for Eurasian grasslands which make up a large portion of the world's grasslands. There is ongoing debate about whether the Eurasian temperate grasslands are C neutral (Hao et al. 2008; Wang et al. 2002). Consequently, long-term, continuous measurements of carbon dioxide (CO_2) flux are crucial to precisely quantify C dynamics in the temperate grassland ecosystems, especially in the context of climate change.

Recently, the eddy covariance (EC) technique has been widely utilized to measure net exchanges of CO_2, water, and energy between vegetation and the atmosphere, with reliable results over various time scales (Baldocchi et al. 2001; Leuning et al. 2005). The fluxes of net ecosystem CO_2 exchange (NEE) measured with micrometeorological methods provide valuable information for understanding photosynthesis as well as respiration at the ecosystem scale (Falge et al. 2002; Sanderman et al. 2003). However, successful application of the EC method requires steady atmospheric conditions, as well as a large footprint, which could limit the utilization of the approach (Baldocchi et al. 2001). In addition, the measured data usually reflect the net C fluxes without distinguishing the specific physiological processes (e.g., autotrophic vs. heterotrophic respiration) underlying the observed NEE variations (Kurbatova et al. 2008). In this study, we tried to overcome the limitation of the EC method by linking measured NEE fluxes to a biogeochemical model, denitrification–decomposition (DNDC), to interpret and integrate the field observations. This paper reports how we adapted the DNDC model based on our own observations and then applied it to predict long-term impacts of climate change on C dynamics in a semiarid grassland in Inner Mongolia, China.

2 Field measurements

2.1 Site description

The eddy tower measurements were conducted in 2004–2005 at the Inner Mongolia Grassland Ecosystem Research Station, one of the stations of China Ecosystem Research Network (CERN) managed by the Chinese Academy of Sciences. The station is located in the Xilin River watershed in the Inner Mongolia Municipality, China (43° 32′N, 116°40′E, 1200 m above sea level; Fig. 1). The study site (400×600 m) is located upon a plat *Leymus chinensis* steppe, which has been fenced off during the past more than 25 years.

The site is within the typical climate zone of semiarid continental temperate steppe, possessing cold and dry winters and warm and moist summers. Snow pack usually covers the soil from the end of November until the end of March. Growing season of the grass lasts about 150–180 days from the end of April to the end of September. During the experimental period, the annual precipitation (rainfall and snowfall) was 394.5 and 163.3 mm for 2004 and 2005, respectively. In 2004, there were 115 days with precipitation including 35 days with the daily precipitation ≥3 mm. In 2005, there were 97 days with precipitation including 14 days with the daily precipitation ≥3 mm (Fig. 2a). The multi-year (1978–2005) average precipitation was 345.4 mm/year (see Fig. 2b).

At the experimental site, the soil is dominated by dark chestnut (Mollisol) with a depth of 100–150 cm (Wang and Cai 1988), containing 21% clay, 60% sand, and 19% silt. There is a litter layer on the soil surface due to accumulation of the grass residue under the fenced condition (i.e., without grazing practice). The volumetric porosity is 0.53 $m^3\ m^{-3}$, the field capacity 0.29 $m^3\ m^{-3}$, and the wilting point 0.12 $m^3\ m^{-3}$ for the top 20 cm soil (see Fig. 2a).

The grassland in the watershed is dominated by C3 annual species. At the experimental site, there were 86 species of flowering plants belonging to 28 families and 67 genera (Jiang 1985). Xeric rhizomatous grass *L. chinensis* is the constructive species with dominant species such as *Agropyron cristatum*, *Cleistogenes squar rosa*, and *Carex duriuscula*. The community coverage index is usually about 25% but could reach to 50% in the wet years (Xiao et al. 1995). The heights of grass clusters are 50–60 cm. The maximum value of leaf area index (LAI) in 2004 (1.54 in August) was approximately two times higher than that in 2005 (0.84 in July; Hao et al. 2008).

The Xilin River watershed is dominated by the grasslands with typical grazing practices. However, the site selected for the study had been treated specially by being fenced without any grazing activity since 1979. This site would provide us an opportunity to observe impact of climate change on the grassland C dynamics without grazing disturbance.

2.2 EC measurements

EC instrument was deployed at the experimental site (see Fig. 1) in April 2003. NEE was measured continuously with the EC system. The fetch from all directions was set to

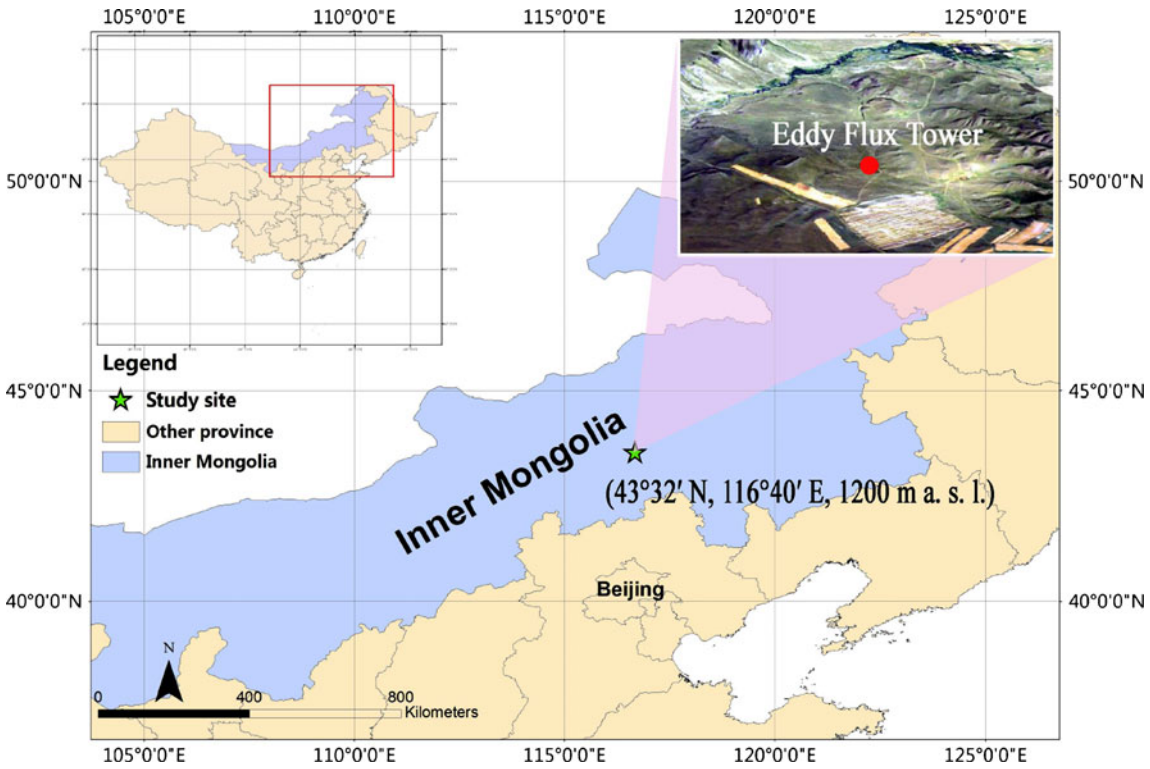

Fig. 1 Location of study sites in an *L. chinensis* steppe in Inner Mongolia, China

be more than 200 m based on the calculation with a footprint model (Kljun et al. 2004). Briefly, a three-axis sonic anemometer (model CSAT3, Campbell Scientific, Mississippi, USA) with an open path infrared CO_2/H_2O gas analyzer (IRGA, LI 7500, LI-COR, Lincoln, NE, USA) was installed at a height of 2.2 m above ground level to measure the fluctuations in three wind components (w, u, v), sensible heat (H), latent heat (LE), and CO_2 fluxes. The instrument provided high-frequency measurements (10 Hz), and the turbulent fluxes data were recorded as half-hour averages by a datalogger (CR5000, Campbell Scientific).

The EC tower was also equipped with instruments to measure the environmental factors used for gap filling calculations: net radiation (CNR-1, Kipp & Zonen, Bohemia, NY, USA), photosynthetically active radiation (PAR; LI-190SB; LI-COR), air temperature and humidity (HMP45C, VAISALA, Woburn, MA, USA). Cup anemometers (034A-L and 014A; Traverse, MI, USA) at 1.5 and 2.5 m above the ground were used to measure wind speed. Precipitation was measured by a tipping bucket rain-gauge (TE525MM, Campbell Scientific) at the height of 1.5 m above the ground level. Soil temperature was measured by copper–constantan thermocouples installed at five depths (0.05, 0.10, 0.20, 0.50, and 1.0 m) below the ground. Soil volumetric water content was measured by time-domain reflectometer (TDR) probes at 0.05, 0.2, and 0.5 m below the ground. All meteorological data from the sensors were collected and stored in a digital datalogger (CR23X; Campbell Scientific). The data measured during 2004–2005 were utilized in the study to support the model simulations.

2.3 Field data processing

Data quality control was implemented to reduce the measurement-induced uncertainties. The collected flux data were adjusted by the Webb, Pearman, and Leuning (WPL) algorithm (Webb et al. 1980). Flux data measured during the rainfall or snowfall events or the instrument malfunctions (e.g., system maintenance, power outages, etc.) were excluded. Since low friction velocity (u*) and weak turbulent mixing tend could result in underestimation of the CO_2 exchange rates (Goulden et al. 1996; Jaksic et al. 2006), only flux data with u* greater than 0.2 m s^{-1} were used. Through screening with the data quality control process, about 20% of the data recorded by the EC system were rejected which led to data gaps. Gap-filling approaches, such as the mean diurnal variation (MDV; Falge et al. 2001) and the interpolation methods developed by (Aubinet et al. 2002; Baldocchi 2003; Baldocchi et al. 2004), were adopted for filling the data gaps in the study. The details of the flux data processing have been described by Hao et al. (2007).

The CO_2 fluxes measured with the EC technique represent NEE, which is the balance between gross primary

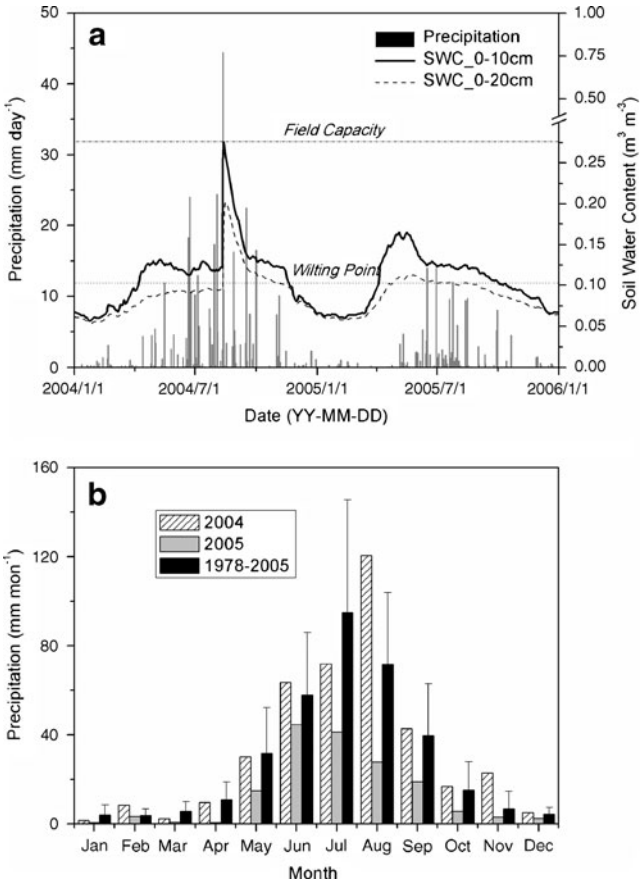

Fig. 2 Seasonal and inter-annual variation in: **a** daily total precipitation and average volumetric soil water content (*SWC*) at 0–10 cm and 0–20 cm soil depths in 2004 and 2005; **b** monthly total precipitation in 2004 and 2005 and means for 1978–2005

productivity (GPP), and ecosystem respiration (R_e; Law et al. 2002). So the value of GPP can be calculated as the difference between R_e and NEE:

$$GPP = R_e - NEE \quad (1)$$

where negative values of NEE indicate net C sequestration by the ecosystem.

Daily R_e is a sum of the daytime ecosystem respiration ($R_{e,\ day}$) and the nighttime ecosystem respiration ($R_{e,\ night}$):

$$R_e = R_{e,day} + R_{e,night}, \quad (2)$$

$R_{e,night}$ is derived from the nighttime net exchange measured with the EC system. Since the $R_{e,night}$ is related to the soil temperature (Kirschbaum 1995), a temperature-dependent model was derived from the measured nighttime average half-hour net CO_2 exchange fluxes ($R_{e,night}$) with soil temperatures as the following:

$$R_{e,night} = ae^{(bTs)}, \quad (3)$$

where T_s represents the soil temperature (°C) at the depth of 0.05 m, and a (μmol of CO_2 m^{-2} s^{-1}) and b (°C) are coefficients.

Thus, by extrapolating the exponential regression correlation to the daytime periods, we estimated the $R_{e,day}$ rates as well as the GPP.

3 Application of the DNDC model

The DNDC model adopted in the study was originally developed for quantifying C sequestration and trace gas emissions from agricultural soils (Li et al. 1992a, b, 1994). The core of DNDC is a soil biogeochemistry model, which can be integrated with different vegetation modules to simulate other ecosystems. In fact, during the past decade, DNDC was further developed to include forest and grassland ecosystems (Hsieh et al. 2005; Kesik et al. 2006; Li et al. 2000; Stange et al. 2000; Xu-Ri et al. 2003). This paper reports a new attempt to test the applicability of DNDC to assess C sequestration for semiarid grassland in China.

The DNDC model consists of two components. The first component, consisting of the soil climate, plant growth and soil organic matter decomposition submodels, predicts soil environmental factors (e.g., soil temperature, moisture, pH, redox potential, and substrate concentration profiles) driven by ecological drivers (e.g., climate, soil, vegetation, and anthropogenic activity). The second component, consisting of the nitrification, denitrification, and fermentation submodels, predicts the emissions of CO_2, methane (CH_4), ammonia (NH_3), nitric oxide (NO), nitrous oxide (N_2O), and dinitrogen (N_2) driven by the soil microbial activities (Li 2007). DNDC simulates C and nitrogen (N) transport and transformation in the plant–soil system in the order "soil climate–plant growth–soil organic matter decomposition–nitrification–denitrification–fermentation" at a daily time step (Li et al. 2000).

In DNDC, the dynamics of soil organic carbon (SOC) is controlled by two major processes, i.e., litter incorporation and SOC decomposition. Rates of both the two processes are determined by the local climate, soil, and management conditions. Since litter production is directly related to the total biomass production of the plants, it is inherently crucial for quantifying litter production to correctly simulate the plant growth. In DNDC, a crop or grass is defined by six parameters, namely, maximum biomass production, biomass partitions to grain, leaf, stem, and root, biomass tissue C/N ratios, accumulative temperature for maturity, water requirement, and N fixation capacity. Equipped with the plant parameters, DNDC simulates the plant growth driven by the air temperature, soil water, and N availabilities at daily time step. If any stress of temperature, water, or N occurs on a day, the biomass production will be accordingly reduced. During the simulated growing seasons, the plant continuously assimilates the atmospheric CO_2 into the biomass C and partitions it to the grain, leaves, stems, and roots every day.

When the plant growth reaches its maturity or the temperature drops below 0°C, the senescence will start. All the root litter will be incorporated in the soil profile and the aboveground residue allocated in the top soil during the senescence. As soon as the fresh litter is incorporated in the soil, the litter will be immediately partitioned into three soil litter pools (i.e., very labile, labile, and resistant litter pools). The soil microbial decomposers use the litter as a source of energy or structural material and, hence, convert the litter to CO_2 and the microbial biomass. After death of the microbes, they will become active humus, which can continue decomposing to become passive humus. During the sequential decomposing processes, part of the organic C becomes CO_2 to be emitted into the atmosphere. If the litter input rate is higher than the bulk decomposition rate, the soil will gain C; otherwise, the soil will become a source of the atmospheric CO_2.

Since this was the first time for DNDC to be applied for C studies for the semiarid grassland in China, we first tested DNDC against part of observed data for calibration. The calibration focused on two groups of input parameters for grass growth and soil hydrology. As most C models, DNDC simulates ecosystem C dynamics by tracking plant growth, litters incorporation, and soil heterotrophic respiration. Since the algorithms of SOC decomposition embedded in DNDC has been calibrated against a number of observations worldwide by many researchers, we did not further calibrate this part anymore. Our calibration effort was focused on the plant growth, as vegetation productivity and phenology could vary greatly from place to place. The physiological and phenology parameters for the grassland simulated in the study were carefully calibrated based on the long term observed datasets of the local grass growth and productivity. As a national experimental station, the Xilinhot site has accumulated records of the local vegetation and management practices. Based on the long-term observations, the grass parameters, such as maximum yield, biomass partitions in the above- and below-ground parts, C/N for the above- and below-ground parts, cumulative thermal degree days, N fixation index, etc., have been thoroughly checked and modified to ensure they could correctly represent the local grass community. In addition, the NEE flux data measured at the experimental site in 2004, a normal year in climate, were also utilized to test the grass simulation and further adjusted some of the grass parameters. The calibrated grass parameters are listed in Table 1 in the manuscript. DNDC simulates soil moisture based on soil hydraulic parameters including porosity, field capacity, wilting point, saturation conductivity, etc. Based on the soil temperature and moisture data observed in 2004, we modified the soil hydraulic parameters to ensure DNDC to correctly simulate the soil moisture profile for the target grassland. After the calibration, the field capacity and wilting point were set to be 0.66 and 0.32, respectively (see details in Table 2).

During the calibration, the statistical tools, the root of mean square error (RMSE), and relative mean deviation (RMD), were utilized to optimize the parameter values based on the comparisons of the modeled results (e.g., biomass partitioning, litter production, NEE fluxes and soil moisture) with the corresponding observations. The calibrations for the Xilinhot grassland ensured the DNDC model to correctly simulate the grass growth and soil climate and hence could estimate the ecosystem C dynamics. In fact, equipped with the calibrated grass and soil parameters linked to the original biogeochemical processes existing in DNDC, the model well captured the depressed grass growth and elevated NEE fluxes in 2005, a dry year.

4 DNDC simulations against observations in 2004 and 2005

In 2004 and 2005, daily C fluxes as well as soil temperature and moisture were measured at the EC tower site. DNDC was run for the same two years to produce the corresponding items. The observed and modeled results were compared to check DNDC's applicability for the Inner Mongolia grassland. Part of the grass and soil moisture data observed in 2004 were utilized for calibrating the grass physiological and phenology parameters as well as the soil hydraulic parameters; however, the modeled results provided a much more comprehensive picture about the carbon and water dynamics for the tested ecosystem, which resulted from the effects of the new parameters in conjunction with the biogeochemical processes (e.g., decomposition, transpiration, evaporation, leaching, etc.) originally existing in DNDC. So the modeled results for both 2004 and 2005 were compared with observations to check the model's behaviors.

4.1 Statistical tools

To quantify the agreement between the simulated and observed results, we adopted three statistical criteria for the validation tests: the coefficient of determination (R^2, Eq. 4), the RMSE (Eq. 5) and the RMD (Eq. 6). Each criterion investigates a specific aspect of the correlation. The R^2 represents a common regression coefficient indicating the ability of the model to explain the variations in the observed values (Janssen and Heuberger 1995). RMSE provides the model's prediction error by heavily weighting high errors. In contrast, RMD weighs all errors the same but tends to smooth out the discrepancies between simulated and observed values. The values of RMD close

Table 1 Physiological and phenology parameters adopted for the experimental grassland in Xilin River watershed in Inner Mongolia, China

Parameter	Value	Unit
Maximum biomass production	4500	kg C/ha/year
Grain fraction of biomass	0.02	–
Leaf and stem fraction of biomass	0.40	–
Root fraction of biomass	0.58	–
C/N ratio of grain	25	–
C/N ratio of leaf and stem	55	–
C/N ratio of root	75	–
Water requirement	250	kg water/kg dry matter
N fixation index	1.50	
Maximum root depth	0.5	M

to 0 indicate the absence of bias in the modeled results (Brisson et al. 2002; Huang et al. 2009). All statistical calculations were performed with a standard statistical analysis software SPSS (Version 13.0, SPSS, Chicago, IL, USA).

$$R^2 = \left(\frac{\sum (O_i - \overline{O})(P_i - \overline{P})}{\sqrt{\sum (O_i - \overline{O})^2 \sum (P_i - \overline{P})^2}} \right)^2, \quad (4)$$

$$RMSE = \sqrt{\frac{\sum_{i=1}^{n} (P_i - O_i)^2}{n}}, \quad (5)$$

$$RMD = \frac{100}{\overline{O}} \sum_{i=1}^{n} \frac{P_i - O_i}{n}, \quad (6)$$

where O_i and P_i represent the observed and model-predicted values, respectively, $\overline{O}$ and $\overline{P}$ are the mean of the observed and predicted values, respectively, and n is the number of observations.

4.2 Comparison on soil climate

Soil temperature and moisture are two primary environmental factors affecting SOC decomposition and also plant growth by altering the soil water and nutrient regimes. Fig. 3a shows comparison between the observed and simulated soil temperatures for the top 0.05 m soil layer. Patterns and magnitudes of the modeled soil temperature were well in agreement with observations. DNDC accurately simulated the trajectories of the observed variations in soil temperature including the temperature effects of the snow pack. The linear regression analysis with the modeled and observed soil temperatures showed a high correlation with R^2=0.96, P<0.0001, RMSE=2.97%, RMD=-29.11% (Table 3). Fig. 3c shows a general clustering of the data with an approximate 1:1 line, although the modeled results slightly underestimated the soil temperature. In addition, the modeled thawing occurred a little later than the observations for 2005 (see Fig. 3a).

Fig. 3b illustrates the comparison of patterns and magnitudes of simulated vs. observed volumetric soil water contents at 0–5 cm depth for the growing season (early April through late September). The simulated soil water contents were in agreement with the field observations. Regression of simulated against observed daily soil moisture data (see Fig. 3d) yielded an R^2 of 0.5, with a slope of 0.85, and an intercept of 0.02 m^3 m^{-3} (n=366, P<0.0001). Values of RMSE and RMD were 0.03% and -0.77%, respectively (see Table 3). In particular, the simulated patterns of soil moisture transition driven by the rainfall events were well consistent

Table 2 Soil property parameters adopted for the experimental grassland in Xilin River watershed in Inner Mongolia, China

Parameters	*L. chinensis* steppe field	Reference
Land-use type	Fenced grassland	(Chen and Wang 2000)
Texture	Dark chestnut (Sandy loam)	(Chen and Wang 2000)
Clay fraction (0–1)	0.21	(Chen and Wang 2000)
Bulk density (g m^{-3})	1.32	(Chen and Wang 2000)
pH	7.56	(Yuan et al. 2008)
Field capacity (wfps, 0–1)	0.66	Observation
Wilting point (wfps, 0–1)	0.32	Observation
Porosity (0–1)	0.53	(Chen and Wang 2000)
SOC at surface soil (0–5 cm) (kg C kg^{-1})	0.015	Observation

wfps Water filled pore space

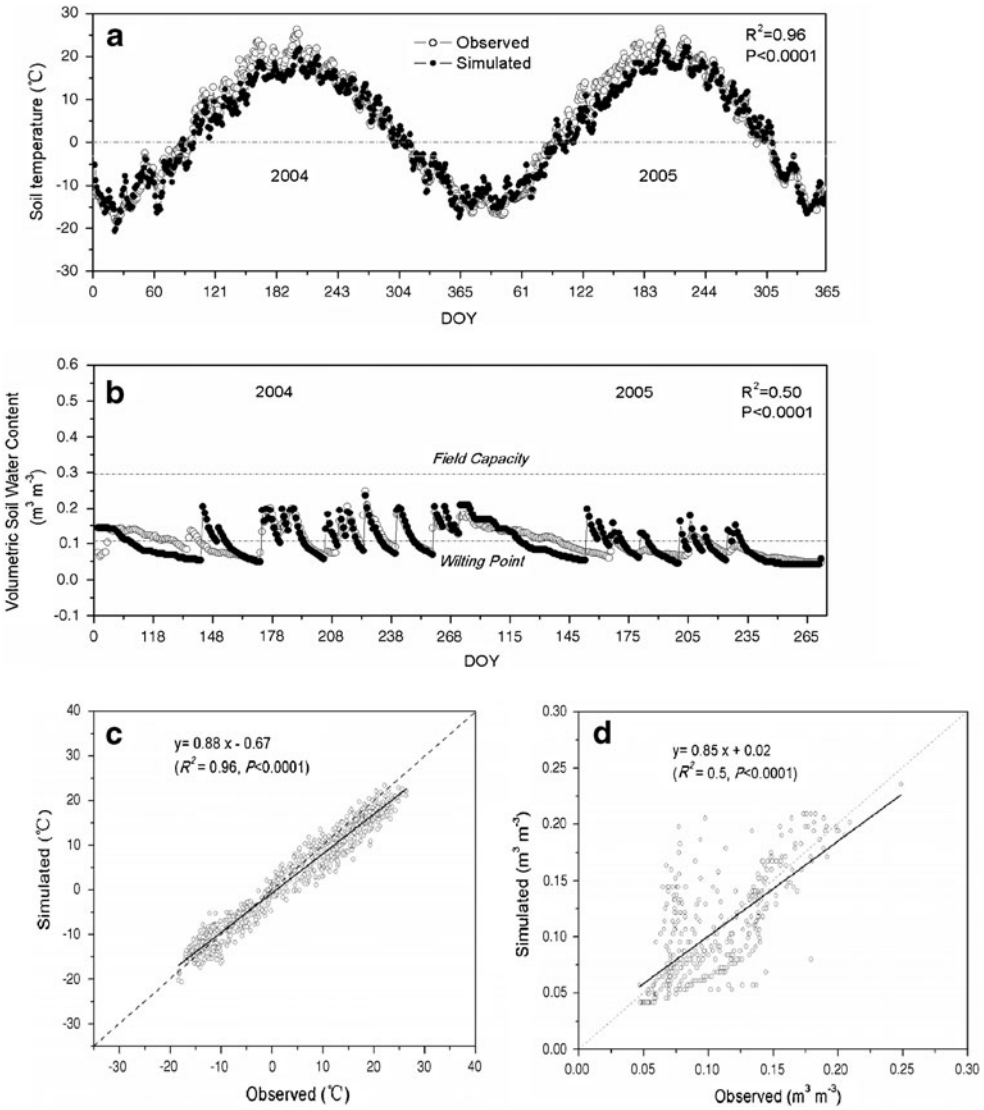

Fig. 3 **a**, **b** Simulated and observed soil surface temperature and volumetric soil water content at 0–5 cm depth, **c**, **d** Simulated vs. observed soil surface temperature and volumetric soil water content at 0–5 cm depth for an *L. chinensis* steppe in Inner Mongolia, China in 2004 and 2005. *Dashed line* is 1:1. *DOY* means day of year

Table 3 Comparisons of simulated and observed daily soil temperature, soil water content, GPP, R_e, NEE, and monthly GPP, R_e, NEE in 2004 and 2005

Crop	Observed vs. simulated	Intercept	Slope	R^2	RMSE (%)	RMD (%)	Number (*n*)
L. chinensis steppe	Soil temperature	-0.67	0.88	0.96*	2.97	-29.11	730
	Soil water content	0.02	0.85	0.50*	0.03	-0.77	366
	Daily GPP	0.58	0.65	0.62*	1.14	3.96	306
	Daily R_e	-0.02	1.00	0.73*	0.56	-0.87	730
	Daily NEE	0.12	0.60	0.36*	0.46	-10.08	730
	Monthly GPP	-0.98	0.89	0.84*	19.19	-5.28	10
	Monthly R_e	-3.09	1.08	0.81*	13.08	-2.20	24
	Monthly NEE	1.44	0.79	0.65*	7.81	-7.37	24

GPP Gross primary productivity, *NEE* net ecosystem CO_2 exchange, R_e ecosystem respiration, R^2 coefficient of determination, *RMD* relative mean deviation, *RMSE* root of mean square error

*Significant at probability level of 0.0001

with observations over the two years (see Fig. 3b). However, the comparison indicated that the modeled soil moistures for 2004 matched observations better than that for 2005. For 2005, an extremely dry year, the model slightly overestimated the elevations of the soil moisture following the rainfall events probably due to underestimation of the actual evapotranspiration (Stange et al. 2000). The discrepancy from our simulation is consistent with the reports from another researcher who indicated that the simulated soil water content was overestimated during the dry period (spring and late autumn) in the typical steppe and the evapotranspiration routines in DNDC would need to be improved for its application for the semiarid grasslands (Xu-Ri et al. 2003).

4.3 Comparison on GPP and R_e

Both the field measurements and the model simulations provided three C fluxes, namely, GPP, R_e (the sum of plant autotrophic respiration and soil microbial heterotrophic respiration), and NEE. Comparisons between the simulated and observed daily GPP fluxes (Fig. 4a, Table 3) indicated that DNDC fairly captured the seasonal variations of observed GPP for the simulated two years. The regression of the simulated vs. observed daily GPP data yielded an R^2 of 0.62 with a slope of 0.65 and an intercept of 0.58 gC m^{-2} day^{-1} ($P<0.0001$; see Table 3). The RMSE and RMD values were 1.14% and 3.96%, respectively. The model commendably captured the U pattern of the plant growth driven by the precipitation variation during the period of July and August in 2004 (see Fig. 4a). Both the modeled and observed data showed that the plant growth was substantially depressed in 2005 due to the long-term droughts. The results proved that DNDC could predict impact of climate change on grass production by precisely capturing the relationships among precipitation, soil moisture, and grass growth. However, DNDC slightly overestimated GPP for the peak-growth season and underestimated GPP for the late growing season of 2005 (see Fig. 4a). To further examine the model performance, we compared the modeled and observed GPP fluxes at a monthly or annual basis (see Table 3). On the monthly basis, there is a significant correlation with an R^2 of 0.84 ($P<0.0001$; see Fig. 4c). At the annual scale, the modeled GPP values were 369.7 and 97.7 gC m^{-2} $year^{-1}$ for 2004 and 2005, separately, while the observed GPP values were 371.2 and 97.2 gC m^{-2} $year^{-1}$ for 2004 and 2005, respectively (Table 4). The modeled and measured annual GPP fluxes are very comparable for both the wet and dry years.

DNDC calculates R_e by simulating plant autotrophic respiration (R_a) and soil microbial heterotrophic respiration (R_h) at daily time step, although the EC method provided only R_e fluxes. Fig. 4a shows the comparison between the simulated and observed R_e data for the tested grassland ecosystem. The modeled daily R_e fluxes are in agreement with observations regarding the patterns and magnitudes (see Fig. 4a, Table 3). The linear regression of simulated against observed daily R_e showed a fairly good correlation ($R^2=0.73$) with a slope of 1.00 and an intercept of -0.02 gC m^{-2} day^{-1} ($P<0.0001$; see Table 3). The values of RMSE and RMD are 0.56% and -0.87%, respectively. However, the model slightly overestimated R_e during the peak-growth season in 2005, an extremely dry year. The simulated and observed peak R_e values were 5.0 and 5.1 gC m^{-2} day^{-1}, respectively, for 2004, while were 3.5 and 2.5 gC m^{-2} day^{-1}, respectively, for 2005 (see Fig. 4a). The discrepancy for 2005 could result from the model's overestimation of the soil water content during the peak-growth season, when the actual soil water content was far below the wilting point (0.12 m^3 m^{-3}; see Fig. 3b).

The monthly R_e fluxes from simulations and observations also showed high correlation (R^2 of 0.81, $P<0.0001$). The modeled annual R_e fluxes were 426 and 284 gC m^{-2} $year^{-1}$ in 2004 and 2005, respectively, which are comparable to the observed R_e fluxes 432 and 294 gC m^{-2} $year^{-1}$ in 2004 and 2005, respectively (see Tables 3 and 4). The modeled results shown in Fig. 4b indicated that R_a and R_h accounted for 46% and 54% of R_e, respectively, in 2004 and 24% and 76% of R_e, respectively, in 2005. The droughts in 2005 apparently depressed both the photosynthesis and respiration of plants at the experimental site.

4.4 Comparison on NEE

The seasonal patterns and magnitudes of simulated daily NEE fluxes were basically in agreement with observations for the period of 2004–2005 (Fig. 5, Table 3). The positive or negative values of NEE in Fig. 5 represent net losses or gains of C, respectively, for the ecosystem. For 2004, the modeled NEE data showed two C loss peaks during the non-growing season (April and October) and two C gain peaks during the growing season (July and August) that was consistent with observations. Based on the statistical analysis on the NEE residuals values, the residuals were not randomly distributed (see Fig. 5b). In absolute magnitude, low NEE residual values were generally associated with low prediction errors of model, whereas high NEE residual values were associated with high prediction errors of model. Moreover, Table 3 depicts the correlation of modeled and observed daily NEE fluxes, which has an R^2 of 0.36 with a slope of 0.60 ($P<0.0001$). The values of RMSE and RMD were 0.46% and -10.8%, respectively. For 2005, DNDC slightly overestimated NEE for the period from 4 June to 12 June (see Fig. 5a) when the model overestimated soil water content (see Fig. 3b) as well as the R_e (see Fig. 4b).

Monthly and annual NEE fluxes were summed based on the daily NEE data over the two years (2004–2005). The patterns and magnitudes of the modeled monthly and annual NEE fluxes were well in agreement with observations (see Fig. 5c). On a monthly scale, the regression of simulated against measured NEE values yielded an R^2 of 0.65 with a slope of 0.79 and an intercept of 1.44 gC m^{-2} mon^{-1} (n=24, P<0.0001; see Table 3), suggesting that the simulated monthly NEE described the measured data better than at the daily time resolution. For the 2004 growing season, the ecosystem was a sink of atmospheric CO_2 with 7.6 or 10.3 gC m^{-2} $year^{-1}$ sequestered based on the modeled or observed data, respectively. In contrast, for the 2005 growing season, the ecosystem was a source of atmospheric CO_2 with 122.5 or 80.2 gC m^{-2} $year^{-1}$ emitted based on the modeled or measured results, respectively (see Table 4). At the annual scale, the simulated annual NEE fluxes were 55.8 and 186.3 gC m^{-2} $year^{-1}$ for 2004 and 2005, respectively, while the observed annual NEE were 82.2 and 179.3 gC m^{-2} $year^{-1}$ for 2004 and 2005, respectively. The results implied that the steppe grassland was a source of atmospheric CO_2 both in 2004 and 2005, although the droughts in 2005 substantially enhanced the C losses from the ecosystem. Nevertheless, the model tended to underestimate NEE in the wet year and slightly overestimate NEE in the dry year. The modeled annual accumulative NEE was

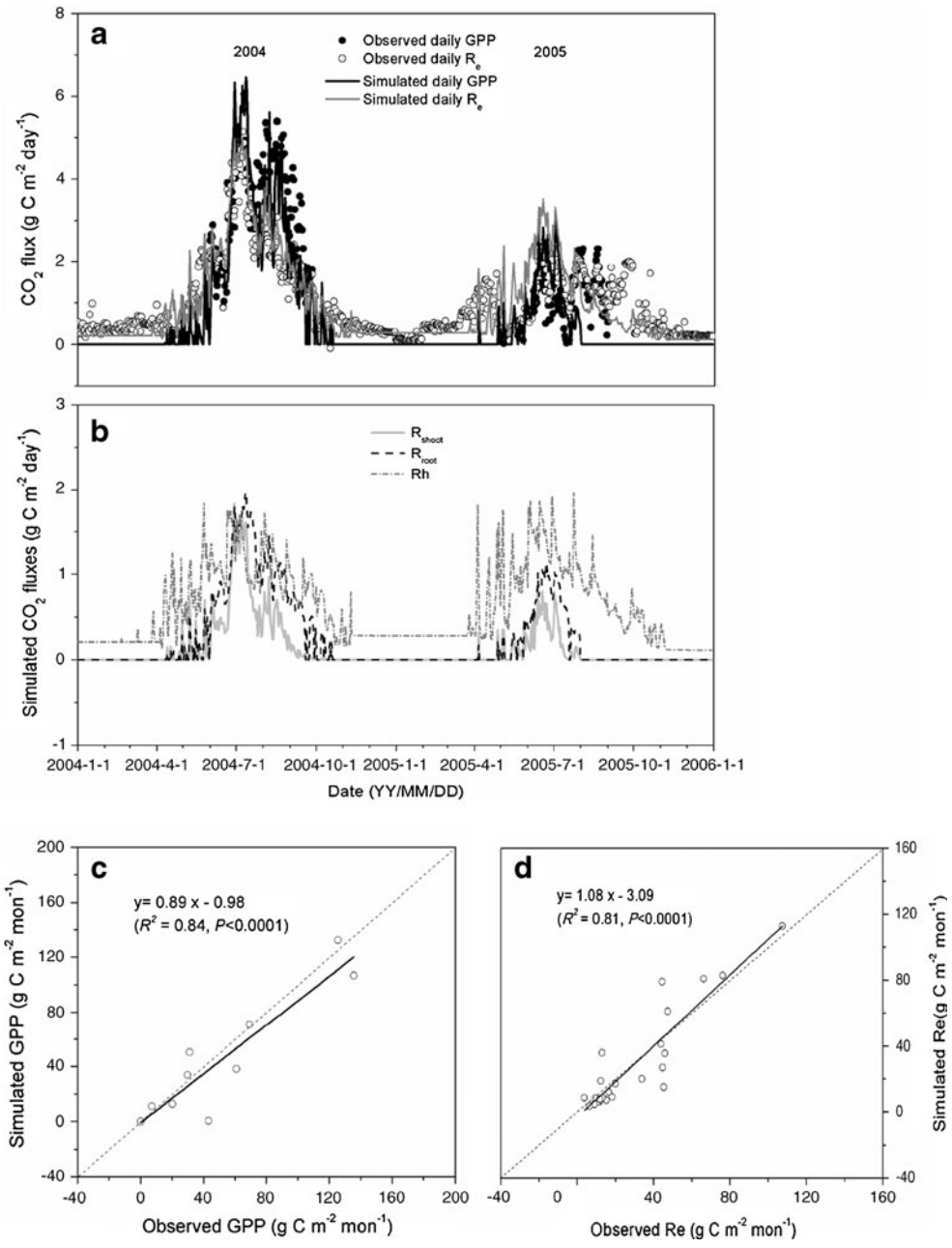

Fig. 4 **a** Comparisons between simulated and observed gross primary productivity (*GPP*) and ecosystem respiration (R_e), **b** Dynamics of simulated shoot respiration (R_{shoot}), root respiration (R_{root}), and soil heterotrophic respiration (R_h), **c**, **d** Simulated vs. observed monthly GPP and Re for an *L. chinensis* steppe in Inner Mongolia, China during 2004–2005. *Dashed line* is 1:1

Table 4 Simulated and observed annual total ecosystem C budget components accumulated from daily simulations and observations for a *L. chinensis* steppe in Inner Mongolia, China over 2004–2005

Item	2004		2005	
	Observed	Simulated	Observed	Simulated
GPP[a]	371.2	369.7	97.2	97.7
R_e	431.8	425.5	293.7	284.0
NEE	82.2	55.8	179.3	186.3
NEE[a]	-10.3	-7.6	80.2	122.5
R_a	–	197.3	–	68.1
R_{shoot}	–	70.4	–	22.7
R_{root}	–	126.9	–	45.3
R_h	–	228.2	–	216.0

GPP Gross primary productivity, R_e ecosystem respiration, *NEE* net ecosystem CO_2 exchange (positive values represent net loss of carbon, negative values represent net gain of carbon), R_a plant autotrophic respiration, R_{shoot} shoot respiration, R_{root} root respiration, R_h soil heterotrophic respiration, – data not available.

[a] During growing season (May to September) only

68% of the observed ones in 2004, while it was 104% in 2005 (see Table 4).

Both the modeled and measured C flux data showed a strong seasonality for this semiarid grassland. Precipitation (including snowfall and rainfall) showed to be a dominant factor affecting the NEE fluxes. Fig. 5a shows high NEE fluxes in April in either 2004 or 2005. According to DNDC model, snowmelt events led to soil moisture elevation and, consequently, stimulated the soil microbial respiration (see Fig. 5a). This may partially explain the sharp increase of CO_2 flux in early spring. After late June in 2004, the grassland ecosystem shifted from a C source to a C sink driven by the increases in GPP following the heavy rainfall events in July and August (see Figs. 2b, 5a). In the 2005 growing season, however, the NEE fluxes were mostly positive values mainly due to the long-term droughts and the low soil moisture status (see Figs. 3b, 5a).

The modeled results showed that soil moisture played a vital role in determining the ecosystem to be a C sink or source as both GPP and R_e can be inhibited by water stress (see Fig. 3b). However, the drought impact looked higher on the grass production than on the soil microbial respiration. The GPP produced in 2004 was about 3.8 times of that in 2005, while the modeled R_h rates differed less between the two years (see Table 4). In general, by comparing the modeled GPP, R_e, and NEE fluxes with observations at daily, monthly, and annual time scales, we gained confidence about the applicability of DNDC for the Chinese grassland in Inner Mongolia.

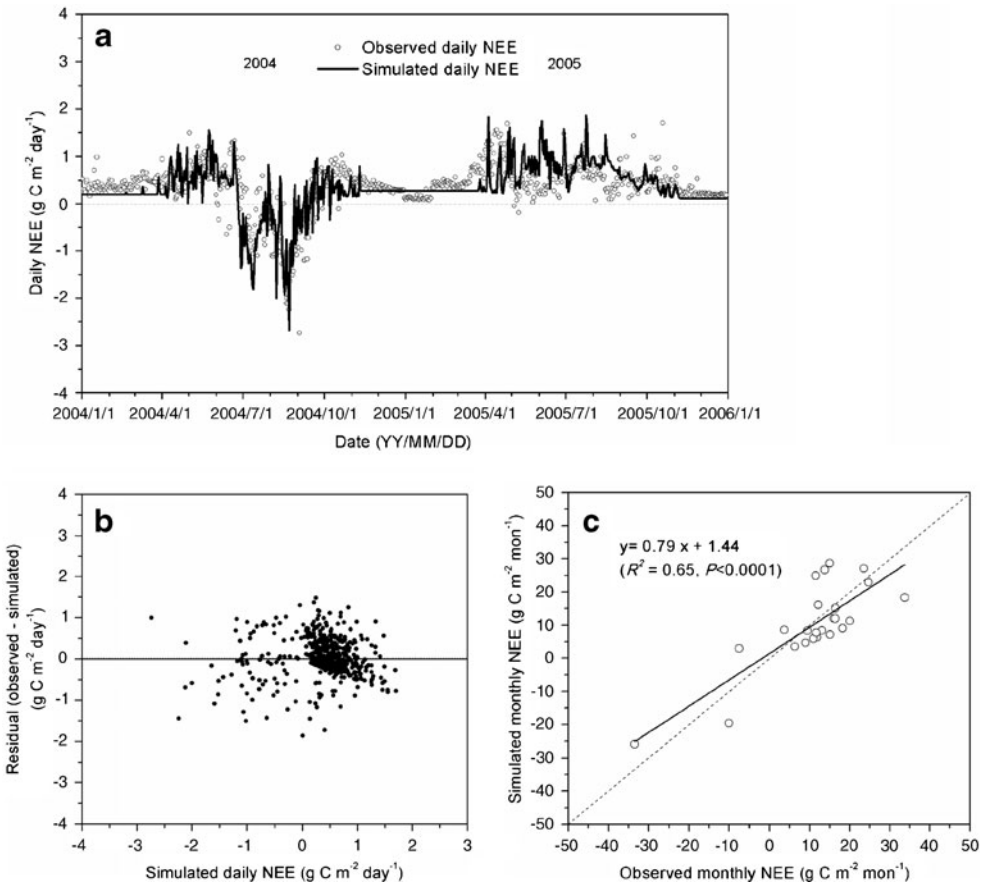

Fig. 5 **a** Comparisons between simulated and observed daily net ecosystem CO_2 exchange (*NEE*), **b** Scatter plot of simulated daily NEE vs. residuals (observed–simulated), **c** Simulated vs. observed monthly NEE for an *L. chinensis* steppe in Inner Mongolia, China during 2004–2005. *Dashed line* is 1:1, where the positive and negative values of NEE represent net loss and gain of carbon (CO_2 fluxes) by the soil–plant–atmosphere system, respectively

5 Estimating impacts of climate change on C dynamics for the grassland

Given the encouraging results from the model validation tests, we decided to utilize the DNDC model for estimating long-term impacts of climate change on C dynamics for the tested grassland in Inner Mongolia, China. A 25-year (1981–2005) daily weather dataset for the very location was obtained from the climate database of our local meteorological station and Inner Mongolia Grassland Ecosystem Research Station, Chinese Academy of Sciences. The 25-year climate data were repeated for four times to create a 100-year climate scenario. The 100-year climate dataset served as a baseline climate scenario for the long-term simulations. Twelve alternative climate scenarios were then composed by varying temperature alone, precipitation alone, or both temperature and precipitation. The alternative climate scenarios were set by decreasing temperature by 4 and 2°C (T1 and T2), increasing temperature by 2 and 4°C (T3 and T4), decreasing precipitation by 40% and 20% (P1 and P2), increasing precipitation by 20% and 40% (P3 and P4), decreasing temperature by 4°C while decreasing precipitation by 40% (T1P1), decreasing temperature by 4°C while increasing precipitation by 40% (T1P4), increasing temperature by 4°C while decreasing precipitation by 40% (T4P1), and increasing temperature by 4°C while increasing precipitation by 40% (T4P4; Table 5). To distinguish the impacts of climate change, we assumed that all other input parameters, such as soil thermo-hydraulic properties and management practices, were kept identical as in the validation tests across the climate scenarios. The grassland was fenced without any grazing activity so that all the plant biomass would be eventually incorporated in the soil. To assess the impacts of the climate alternatives on the grassland C dynamics, the simulated annual plant production, soil heterotrophic respiration, and net change in SOC storage were recorded as three indicators to represent the input C flux, output C flux, and net C flux for the modeled soil.

By running DNDC with the 100-year baseline climate scenario, we obtained annual grass yield, soil heterotrophic CO_2 flux, and net change in SOC content for each year. Fig. 6 shows the modeled results. The annual grass production varied between 200 and 3,500 kg C/ha/year driven mainly by the interannual variations in precipitation, while the soil CO_2 fluxes varied moderately. The annual litter incorporation dominated the SOC dynamics for the grassland. During the wet years, the grass yields were high, and the soil gained more C by having more litter incorporated. In contrast, in the dry years with poor biomass production, the SOC decomposition rates were higher than the litter incorporation rates that led to a net loss in the SOC storage. In general, the modeled results indicated that the fenced grassland sequestered C at an average rate of 210 kg C/ha/year under the baseline climate conditions during the simulated 100 years. The results imply that the grassland would be a sink of atmosphric CO_2 under the current climate conditions if the land will be continuously fenced without any grazing activities.

Simulations with the 12 alternative climate scenarios were conducted to assess their impacts on the grass production as well as the SOC storage. DNDC estimates the impact of climate on plant growth by tracking the temperature stress and water stress. When temperature or precipitation changes, the change will alter the soil temperature and moisture regimes and, hence, affect a series of soil processes including transpiration, evaporation, decomposition, nitrification, denitrification, etc., which eventually change the availability of water or nutrients for the plants growing on the soil. The change in plant biomass production will determine the litter incorporation and, hence, alter the SOC dynamics. Table 6 provides all the simulated results of temperature stress, water stress, grass production, and change in SOC storage under the baseline and alternative climate conditions for the target grassland in Inner Mongolia.

Table 5 Alternative climate scenarios for predicting impacts of climate change on C dynamics in the grassland in Inner Mongolia, China

	Change in air temperature (°C)					
Change in precipitation		-4	-2	0	+2	+4
	60%	T1P1		P1		T4P1
	80%			P2		
	100%	T1	T2	Base	T3	T4
	120%			P3		
	160%	T1P4		P4		T4P4

T1 Decrease in temperature by 4°C, *T2* decrease in temperature by 2°C, *T3* increase in temperature by 2°C, *T4* increase in temperature by 4°C, *P1* decrease in precipitation by 40%, *P2* decrease in precipitation by 20%, *P3* increase in precipitation by 20%, *P4* increase in precipitation by 40%, *T1P1* decrease in temperature by 4°C while decrease in precipitation by 40%, *T1P4* decrease in temperature by 4°C while increase in precipitation by 40%, *T4P1* increase in temperature by 4°C while decrease in precipitation by 40%, *T4P4* increase in temperature by 4°C while increase in precipitation by 40%

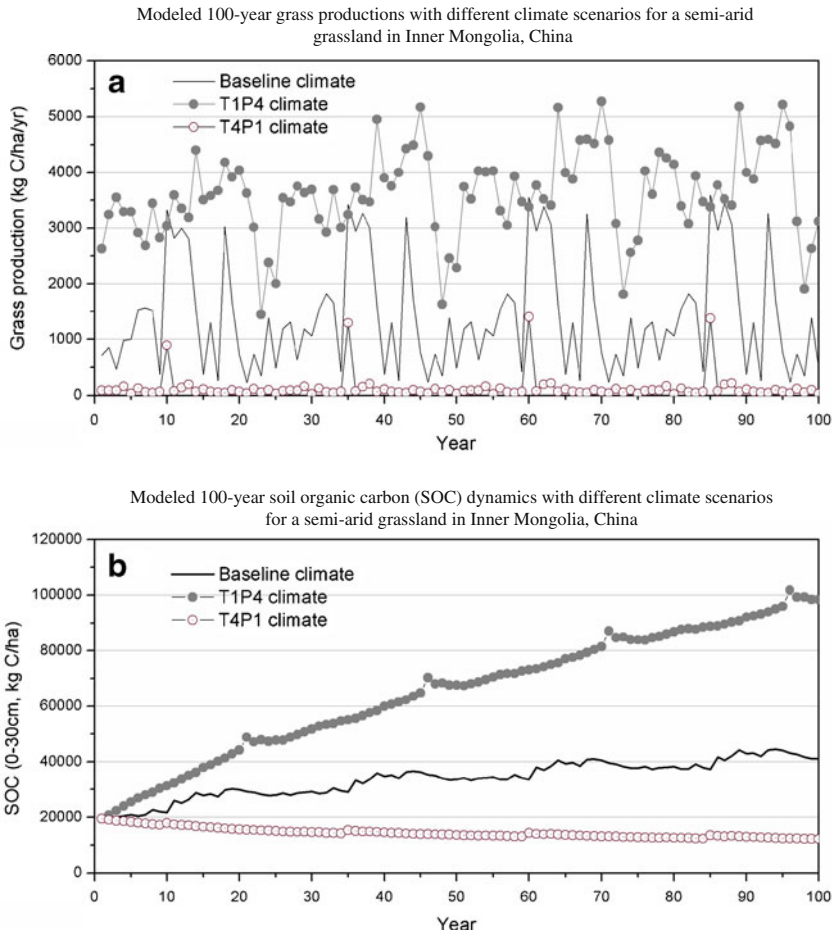

Fig. 6 DNDC-modeled biomass productions (**a**) and SOC dynamics (**b**) in a fenced grassland in Inner Mongolia, China under current (*Baseline*), cooler and wetter (*T1P4*), and warmer and drier (*T4P1*) climate conditions in the coming 100 years

Scenarios T1, T2, T3, and T4 represent the future climate conditions with change in sole temperature. T1 or T2 is the cooler scenario with the daily air temperatures decreased by 4 or 2°C; while T3 or T4 the warmer scenario with the daily air temperatures increased by 2 or 4°C. The modeled results indicated that when the climate became cooler, the crop water stress got improved that elevated the grass yield and finally increased the soil C sequestration

Table 6 100-year mean annual grass production, SOC change, and temperature and water stress indices from DNDC simulations with baseline and alternative climate scenarios

Climate scenario	Grass production (kg C/ha/year)	Change in SOC (kg C/ha/year)	Temperature stress index[a]	Water stress index[a]
Baseline	1,414	211	0.99	0.74
T1	2,214	377	0.63	0.90
T2	2,300	389	0.82	0.82
T3	768	48	1.00	0.67
T4	491	-22	1.00	0.60
P1	267	-53	0.99	0.64
P2	703	8	0.99	0.69
P3	2,331	503	0.99	0.80
P4	3,150	835	0.99	0.85
T1P1	634	0	0.63	0.77
T1P4	3,598	789	0.63	0.97
T4P1	133	-72	1.00	0.54
T4P4	1,227	199	1.00	0.69

[a] Temperature or water stress index: *1* No stress, *0* severe stress

rates from the baseline 200–380 kg C/ha/year. In contrast, the increases in temperature enhanced the water stress, substantially decreased the grass yield, and turned the soil to a very weak sink and even a source of atmospheric C in the future 100 years (see Table 6).

Scenarios P1, P2, P3, and P4 represent the future climate conditions with change in sole precipitation. P1 or P2 is the drier scenario with the annual precipitation decreased by 40% or 20%; while P3 or P4 the more moist scenario with the precipitation increased by 20% or 40%, respectively. The modeled results indicated that when the climate became drier, the crop water stress became worse that it severely decreased the grass yield as well as the soil C sequestration capacity. In contrast, the increases in precipitation substantially increased the grass yield and increased the soil C sequestration rates as high as 2.4–4.0 times of the baseline rate in the future 100 years (see Table 6).

The scenarios T1P1, T1P4, T4P1, and T4P4 represent for climate conditions by combining the changes in both temperature and precipitation. The warmer and drier climate scenario (i.e., T4P1) made the worst case having the lowest grass production (only 133 kg C/ha/year) with 72 kg C/ha/year lost from the SOC pool; the cooler and wetter climate scenario (T1P4) made the best case having the highest biomass production (3,600 kg C/ha/year) with 790 kg C/ha/year sequestered in the soil during the simulated 100 years.

In summary, based on the 100-year simulations with the baseline and alternative climate conditions, the studied grassland would gain C due to the conservative management practices (i.e., fenced with no grazing). Since the ecosystem production is precipitation-limited, a cooler or wetter future climate would substantially elevate the C sequestration capacity of the grassland. However, if the future climate turns to be drier and/or warmer, the C sequestration potential would significantly decrease and even become negative to turn the ecosystem to a source of atmospheric CO_2.

6 Discussions

Due to the rising of atmospheric concentrations of greenhouse gases, global mean surface temperature is projected to increase between 1.8 and 4.0°C over the next 100 years, and precipitation is highly variable spatially and temporally (IPCC 2007). These climate changes will alter the C budget in the semiarid grassland ecosystems, most of which are vulnerable to the soil water deficits (Houborg and Soegaard 2004). Since a large portion of Chinese grasslands are located in the semiarid climatic zones, we selected a typical grassland in the Xilin River watershed in Inner Mongolia as a representative to study its C dynamics with a modeling approach. The DNDC model adopted in the study has a relatively complete set of biogeochemical processes embedded in the model framework, which integrate climate, soil, vegetation, and management practices by precisely tracking their interactions within the ecosystems (Li 2007; Li et al. 1992a, b). During nearly the past 20 years, DNDC has been independently tested by a large number of researchers worldwide with encouraging results on both C sequestration and trace gas emissions (see a summary in Giltrap et al. 2010). We further tested the model against our own datasets measured at the Xilin grassland site. Satisfied with the validation tests, especially regarding the responses of the modeled NEE fluxes to the climate variation, we utilized DNDC to estimate the impacts of several assumed future climate scenarios on C dynamics for the target grassland. We realized that the current grassland production as well as SOC dynamics in China are affected by a number of factors including climate change and land-use management. However, to identify the impact of sole climate change, we selected a grassland with the least human's disturbance, which was fenced for many years with no grazing activity. The modeled results indicated that, even for such a grassland with very conservative management practices, it could still become a source of atmospheric CO_2 if the local climate turns to be warmer and drier. This case study would set a baseline of C dynamics for most semiarid grasslands in China. As a large portion of the Chinese grasslands are suffering not only from climate change but also from imperfect management practices such as over-grazing and removal of manure, the SOC losses from the grassland ecosystems could be much faster than the modeled results in the study if the worse scenarios of climate change occur. Following the study reported in this paper, we will continue utilizing the modeling approach to explore alternative management opportunities, such as fertilization, reduced grazing, etc., to find out to what degree we could moderate the negative effects of climate change through improving our grassland management practice.

Acknowledgements The study reported in this paper was supported by the major research plan organized by the National Natural Science Foundation of China (90711001). The participation of Changsheng Li in the study was supported by NSF Biocomplexity in the Environment/ Coupled Natural-Human Cycles Program (0508028) and NASA Terrestrial Ecology project "Modeling carbon dynamics in high latitude wetlands" (NNX09AQ36G). We thank the two anonymous reviewers for their valuable comments and suggestions on the earlier versions of the manuscript. The authors also would like to thank Ri Xu, Zaixing Zhou, and Ligang Wang for their help.

References

Aubinet M, Heinesch B, Longdoz B (2002) Estimation of the carbon sequestration by a heterogeneous forest: night flux corrections, heterogeneity of the site and inter-annual variability. Glob Chang Biol 8:1053–1071

Baldocchi DD (2003) Assessing the eddy covariance technique for evaluating carbon dioxide exchange rates of ecosystems: past, present and future. Glob Chang Biol 9:479–492

Baldocchi D, Falge E, Gu LH, Olson R, Hollinger D, Running S, Anthoni P, Bernhofer C, Davis K, Evans R, Fuentes J, Goldstein A, Katul G, Law B, Lee XH, Malhi Y, Meyers T, Munger W, Oechel W, KTP U, Pilegaard K, Schmid HP, Valentini R, Verma S, Vesala T, Wilson K, Wofsy S (2001) FLUXNET: a new tool to study the temporal and spatial variability of ecosystem-scale carbon dioxide, water vapor, and energy flux densities. Bull Am Meteorol Soc 82:2415–2434

Baldocchi DD, Xu LK, Kiang N (2004) How plant functional-type, weather, seasonal drought, and soil physical properties alter water and energy fluxes of an oak-grass savanna and an annual grassland. Agric For Meteorol 123:13–39

Brisson N, Ruget F, Gate P, Lorgeau J, Nicoullaud B, Tayot X, Plenet D, Jeuffroy MH, Bouthier A, Ripoche D, Mary B, Justes E (2002) STICS: a generic model for simulating crops and their water and nitrogen balances. II. Model validation for wheat and maize. Agronomie 22:69–92

Chen ZZ, Wang SP (2000) Chinese typical grassland ecosystem. Science Press, Beijing

Falge E, Baldocchi D, Olson R, Anthoni P, Aubinet M, Bernhofer C, Burba G, Ceulemans R, Clement R, Dolman H, Granier A, Gross P, Grunwald T, Hollinger D, Jensen NO, Katul G, Keronen P, Kowalski A, Lai CT, Law BE, Meyers T, Moncrieff H, Moors E, Munger JW, Pilegaard K, Rannik U, Rebmann C, Suyker A, Tenhunen J, Tu K, Verma S, Vesala T, Wilson K, Wofsy S (2001) Gap filling strategies for defensible annual sums of net ecosystem exchange. Agric For Meteorol 107:43–69

Falge E, Baldocchi D, Tenhunen J, Aubinet M, Bakwin P, Berbigier P, Bernhofer C, Burba G, Clement R, Davis KJ, Elbers JA, Goldstein AH, Grelle A, Granier A, Guomundsson J, Hollinger D, Kowalski AS, Katul G, Law BE, Malhi Y, Meyers T, Monson RK, Munger JW, Oechel W, Paw KT, Pilegaard K, Rannik U, Rebmann C, Suyker A, Valentini R, Wilson K, Wofsy S (2002) Seasonality of ecosystem respiration and gross primary production as derived from FLUXNET measurements. Agric For Meteorol 113:53–74

Fan S, Gloor M, Mahlman J, Pacala S, Sarmiento J, Takahashi T, Tans P (1998) A large terrestrial carbon sink in North America implied by atmospheric and oceanic carbon dioxide data and models. Science 282:442–446

Giltrap DL, Li CS, Saggar S (2010) DNDC: a process-based model of greenhouse gas fluxes from agricultural soils. Agric Ecosyst Environ 136:292–300

Goulden ML, Munger JW, Fan SM, Daube BC, Wofsy SC (1996) Measurements of carbon sequestration by long-term eddy covariance: methods and a critical evaluation of accuracy. Glob Chang Biol 2:169–182

Hao YB, Wang YF, Huang XZ, Cui XY, Zhou XQ, Wang SP, Niu HS, Jiang GM (2007) Seasonal and interannual variation in water vapor and energy exchange over a typical steppe in Inner Mongolia, China. Agric For Meteorol 146:57–69

Hao YB, Wang YF, Mei XR, Huang XZ, Cui XY, Zhou XQ, Niu HS (2008) CO_2, H_2O and energy exchange of an Inner Mongolia steppe ecosystem during a dry and wet year. Acta Oecol 33:133–143

Houborg RM, Soegaard H (2004) Regional simulation of ecosystem CO_2 and water vapor exchange for agricultural land using NOAA AVHRR and Terra MODIS satellite data. Application to Zealand, Denmark. Remote Sens Environ 93:150–167

Hsieh CI, Leahy P, Kiely G, Li CS (2005) The effect of future climate perturbations on N_2O emissions from a fertilized humid grassland. Nutr Cycl Agroecosyst 73:15–23

Huang Y, Yu YQ, Zhang W, Sun WJ, Liu SL, Jiang J, Wu JS, Yu WT, Wang Y, Yang ZF (2009) Agro-C: a biogeophysical model for simulating the carbon budget of agroecosystems. Agric For Meteorol 149:106–129

Hunt JE, Kelliher FM, McSeveny TM, Ross DJ, Whitehead D (2004) Long-term carbon exchange in a sparse, seasonally dry tussock grassland. Glob Chang Biol 10:1785–1800

IPCC (2007) Climate change 2007: the physical science basis. Contribution of Working Group I to the fourth assessment report of the intergovernmental panel on climate change. Cambridge University Press, Cambridge

Jaksic V, Kiely G, Albertson J, Oren R, Katul G, Leahy P, Byrne KA (2006) Net ecosystem exchange of grassland in contrasting wet and dry years. Agric For Meteorol 139:323–334

Janssen PHM, Heuberger PSC (1995) Calibration of process-oriented models. Ecol Model 83:55–66

Jiang S (1985) An introduction on the inner mongolia grassland ecosystem research station. Academia Sinica. Inner mongolia grassland ecosystem research station. Res Grassland Ecosyst 1:1–10

Kesik M, Bruggemann N, Forkel R, Kiese R, Knoche R, Li CS, Seufert G, Simpson D, Butterbach-Bahl K (2006) Future scenarios of N_2O and NO emissions from European forest soils. J Geophys Res 111

Kirschbaum MUF (1995) The temperature-dependence of soil organic-matter decomposition, and the effect of global warming on soil organic-C storage. Soil Biol Biochem 27:753–760

Kljun N, Calanca P, Rotachhi MW, Schmid HP (2004) A simple parameterisation for flux footprint predictions. Boundary-Layer Meteorol 112:503–523

Kurbatova J, Li CS, Varlagin A, Xiao XM, Vygodskaya N (2008) Modeling carbon dynamics in two adjacent spruce forests with different soil conditions in Russia. Biogeosciences 5:969–980

Law BE, Falge E, Gu L, Baldocchi DD, Bakwin P, Berbigier P, Davis K, Dolman AJ, Falk M, Fuentes JD, Goldstein A, Granier A, Grelle A, Hollinger D, Janssens IA, Jarvis P, Jensen NO, Katul G, Mahli Y, Matteucci G, Meyers T, Monson R, Munger W, Oechel W, Olson R, Pilegaard K, Paw KT, Thorgeirsson H, Valentini R, Verma S, Vesala T, Wilson K, Wofsy S (2002) Environmental controls over carbon dioxide and water vapor exchange of terrestrial vegetation. Agric For Meteorol 113:97–120

Leuning R, Cleugh HA, Zegelin SJ, Hughes D (2005) Carbon and water fluxes over a temperate Eucalyptus forest and a tropical wet/dry savanna in Australia: measurements and comparison with MODIS remote sensing estimates. Agric For Meteorol 129:151–173

Li CS (2007) Selenium deficiency and endemic heart failure in China: a case study of biogeochemistry for human health. Ambio 36:90–93

Li CS, Frolking S, Frolking TA (1992a) A model of nitrous-oxide evolution from soil driven by rainfall events: 1. Model structure and sensitivity. J Geophys Res 97:9759–9776

Li CS, Frolking S, Frolking TA (1992b) A model of nitrous-oxide evolution from soil driven by rainfall events: 2. Model applications. J Geophys Res 97:9777–9783

Li CS, Frolking S, Harriss R (1994) Modeling carbon biogeochemistry in agricultural soils. Glob Biogeochem Cycles 8:237–254

Li CS, Aber J, Stange F, Butterbach-Bahl K, Papen H (2000) A process–oriented model of N_2O and NO emissions from forest soils: 1. Model development. J Geophys Res 105:4369–4384

Meyers TP (2001) A comparison of summertime water and CO_2 fluxes over rangeland for well watered and drought conditions. Agric For Meteorol 106:205–214

Nagy Z, Pinter K, Czobel S, Balogh J, Horvath L, Foti S, Barcza Z, Weidinger T, Csintalan Z, Dinh NQ, Grosz B, Tuba Z (2007) The carbon budget of semi-arid grassland in a wet and a dry year in Hungary. Agric Ecosyst Environ 121:21–29

Sanderman J, Amundson RG, Baldocchi DD (2003) Application of eddy covariance measurements to the temperature dependence of soil organic matter mean residence time. Glob Biogeochem Cycles 17:15

Sims PL, Bradford JA (2001) Carbon dioxide fluxes in a southern plains prairie. Agric For Meteorol 109:117–134

Stange F, Butterbach-Bahl K, Papen H, Zechmeister-Boltenstern S, Li CS, Aber J (2000) A process-oriented model of N_2O and NO emissions from forest soils 2. Sensitivity analysis and validation. J Geophys Res 105:4385–4398

Sundquist ET (1993) The global carbon-dioxide budget. Science 259:934–941

Suyker AE, Verma SB, Burba GG (2003) Interannual variability in net CO_2 exchange of a native tallgrass prairie. Glob Chang Biol 9:255–265

Tans PP, Fung IY, Takahashi T (1990) Observational constraints on the global atmospheric CO_2 budget. Science 247:1431–1438

Wang JW, Cai C (1988) Studies on genesis, types and characteristics of the soils of the Xilin River Basin. In: Inner Mongolia Grassland Ecosystem Research Station (ed.). Res Grassland Ecosyst 3:23–83

Wang GX, Qian J, Cheng GD, Lai YM (2002) Soil organic carbon pool of grassland soils on the Qinghai-Tibetan Plateau and its global implication. Sci Total Environ 291:207–217

Webb EK, Pearman GI, Leuning R (1980) Correction of flux measurements for density effects due to heat and water-vapor transfer. Q J R Meteorol Soc 106:85–100

Xiao XM, Wang YF, Jiang S, Ojima DS, Bonham CD (1995) Interannual variation in the climate and above-ground biomass of *Leymus chinensis* steppe and Stipa grandis steppe in the Xilin River Basin, Inner Mongolia, China. J Arid Environ 31:283–299

Xu LK, Baldocchi DD (2004) Seasonal variation in carbon dioxide exchange over a Mediterranean annual grassland in California. Agric For Meteorol 123:79–96

Xu-Ri WYS, Zheng XH, Ji BM, Wang MX (2003) A comparison between measured and modeled N_2O emissions from Inner Mongolian semi-arid grassland. Plant Soil 255:513–528

Yuan F, Han XG, Ge JP, Wu JG (2008) Net primary productivity of *Leymus chinensis* steppe in Xilin River Basin of Inner Mongolia and its responses to global climate change. Chin J Appl Ecol 19:2168–2176

Zhang L, Wylie BK, Ji L, Gilmanov TG, Tieszen LL (2010) Climate-driven interannual variability in net ecosystem exchange in the Northern Great Plains Grasslands. Rangeland Ecol Manag 63:40–50